4^{th} Int. Conf. on Advanced A/D and D/A Conversion Techniques and their Applications,
7^{th} European Workshop on ADC Modelling and Testing,
June 26-28, 2002, Prague, Czech Republic

Testing ADCs for Static and Dynamic Nonlinearities —Killing two birds with one stone—

Carsten Wegener and Michael Peter Kennedy
Dept. of Microelectronic Engineering University College Cork, Ireland
Tel.: +353 21 4904572, FAX: +353 21 4904573
email: carsten_wegener@email.com, Peter.Kennedy@ucc.ie

***Abstract** – Traditionally, static linearity and dynamic distortion tests are performed separately for ADCs. To this end, a low-frequency sine-wave is histogrammed to measure static Integral Nonlinearity, and a high-frequency sine-wave is sampled for FFT processing to measure dynamic distortions and dynamic range.*

We propose to use a model-based technique to extract both static and dynamic nonlinearities from a single data record of a sampled high-frequency sine-wave. This saves test time as the ADC converts fewer samples.

***Keywords** – ADC testing, histogram, FFT, static and dynamic nonlinearities*

I. Introduction

As the specifications for ADCs improve due to technology and design advances, for commodity parts like low-power, medium speed, SAR-type converters the test costs constitute an increasing proportion of the total product costs. To reduce these costs it is required to maximize the information gained from the measurements performed on the device under test (DUT).

In this work we report how we have modified a test time reduction technique that has been shown to reduce the measurement effort for histogram based testing of static Integral Nonlinearity (INL) specifications for Nyquist rate ADCs [1]. Instead of converting a slow sine-wave for static INL testing [2] and a fast sine-wave for dynamic distortion and SNR testing [3], we suggest to convert only the fast sine-wave, and to extract both specifications from this measurement.

The conversion result of the fast sine-wave can directly be used for FFT analysis to determine if the DUT meets the dynamic test specifications. From the conversion result we can also form a histogram of the ADC output codes to obtain a "dynamic INL" which itself might be a specification depending on the application area of the ADC [4].

Static INL tests usually over-drive the ADC input by about 5% to accommodate for gain and offset errors. Overdriving the ADC input can seriously upset the converter dynamics in a complicated way, and should therefore be avoided. With our approach we can choose to use a sine-wave input that covers slightly less than the allowable ADC input range, which on the one hand is compatible with dynamic SNR and distortion tests and on the other hand avoids overdriving the ADC.

From the results for a set of $N = 77$ devices, we found that this model-based test technique derives from the dynamic INL measurement an approximation of the static INL at all codes that is more accurate than if we measure the static INL directly, taking the same number of samples. This comes somewhat as a surprise, but is due to the model averaging out measurement noise and the test setup for the fast sine-wave presenting the ADC with a less noisy signal using a high-quality band-pass filter in the signal path.

The authors acknowledge support by Enterprise Ireland and Analog Devices B.V.

II. Model-based testing of INL

Model-based testing has been developed over the past two decades at the National Institute of Standards and Technology (NIST) [5], [6], at Eindhoven University supported by Philips [7], at Stanford University supported by National Semiconductor [1], at the National University of Ireland supported by Analog Devices [8], [9] and at Georgia Institute of Technology supported by National Semiconductor [10].

A. Model building

The INL characteristic of a device is written as a column vector b with 8192 elements: the top 4096 elements contain the INL values per code under static input conditions,[1] and the bottom 4096 elements are determined under dynamic input conditions.[2] Taylor expansion of this vector valued function around b_0, which denotes the typical INL characteristic, yields a linear model

$$b - b_0 \approx Ax, \tag{1}$$

where A is called the *model matrix*, and x is called the *model parameter vector.* The number of columns of A and the number of elements in x necessarily coincide and

[1] Obtained by histogramming a 50 Hz sine-wave[3].
[2] Obtained by histogramming a 100 kHz sine-wave[3].

we refer to it as the *model order* denoted in the following by n.

Based on a set of fully and accurately[3] measured devices we develop the linear model A. To this end, we form a matrix B with one column per device, and one row per test point on a device. For our set of 77 devices with 12-bit resolution at 600 kSamples/s throughput, we have measured static INL and dynamic INL characteristics. The typical characteristic b_0 is determined by taking the row-mean of B. The static part of this INL characteristic is shown in Fig. 1(a) for our device type. In part (b) of the same figure, we show the typical INL difference between static and dynamic input conditions. The magnitude of this difference indicates a significant shift of the INL characteristic when changing test conditions.

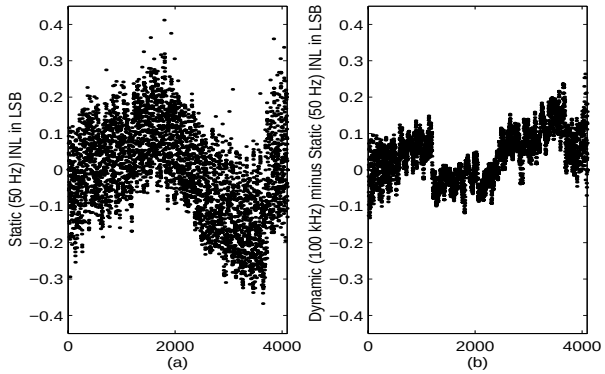

Fig. 1. (a) Typical static INL versus code, and (b) typical difference in INL measurement for static (50 Hz) and dynamic (100 kHz) inputs.

To obtain the model matrix A in (1), we apply Singular Value Decomposition [11]

$$B - B_0 = U\Sigma V^T, \tag{2}$$

where B_0 is formed by replicating the column vector b_0. For a given model order n we use the first n columns of U as the model matrix A [6]. For each device under test on the production line, we solve (1) in the least-squares sense for x. Having determined x, we calculate the predicted device characteristic as $\hat{b} = b_0 + Ax$. Note that the set of linear equations in (1) is over-determined; thus, it is possible to save measurement effort by measuring only a subset of the INL test points.

B. Model order selection

The quality of a model is measured in terms of the difference between the predicted characteristic $\hat{b}$ and the true characteristic b of a device that is not part of the modeling set. For conciseness, we introduce the maximum "prediction error"

$$e_{\max} = \underset{i=1,\ldots,N}{\text{mean}} \left(\|\hat{b}^i - b^i\|_\infty\right) + 3 \cdot \underset{i=1,\ldots,N}{\text{std}} \left(\|\hat{b}^i - b^i\|_\infty\right) \tag{3}$$

evaluated over a set of N devices. Moreover, we define the rms-prediction error e_{rms} similar to (3) by replacing the infinity norm with the root-mean-square (rms) norm.

When evaluating $e_{\max}$ and e_{rms} respectively, over our set of $N = 77$ devices, we determine $\hat{b}$ based on a model built from the remaining 76 devices. This technique is termed in [12] as "delete-one-cross-correlation." The prediction error is influenced by

- measurement noise present in production,
- the test points selected to determine x, and
- non-modeled device behavior.

The determination of an appropriate model order n is a trade-off between computational effort on the production line (which increases linearly with n) and non-modeled device behavior. To estimate non-modeled behavior, we use all possible test points when solving (1) for x and predicting $\hat{b}$ for use in (3). In Fig. 2, we show the prediction error versus model order n and observe a lower boundary for n beyond which too little an improvement in terms of prediction error is achieved despite an increase in model order. This characterizes the optimal model order $n = 40$ which we will use in the following.

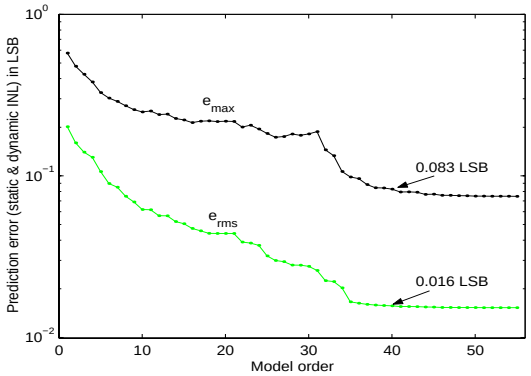

Fig. 2. Prediction error $e_{\max}$ (in black) and e_{rms} (in gray) versus model order n using all test points of "true" device characteristics.

C. Test point selection

We select test points at which the device characteristics are measured on the production line. The more test points we select, the larger the set of equations in (1) that we solve for x. The larger the number of equations the larger the computational effort, and the more over-determined is the set of equations. An over-determined set of equations can reduce the impact of measurement noise on the estimated model parameter vector x.

For the modeling set of devices, we also collect production type measurements in a matrix $\tilde{B}$. From

[3] We use averaging of repeated measurements to reduce noise-induced uncertainties.

the difference $\tilde{B} - B$ we estimate the magnitude of the noise at each of the test points. In Fig. 3, we plot in gray the standard deviation of the rows of $\tilde{B} - B$ versus the corresponding ADC output code. By construction, the end points of the INL characteristics are noise-free. For the inner test points (codes 1 through 4094), the plots suggest an underlying bow-shape which is due to the sine-wave input signal and its probability density over the converter input range. We have fitted a second-order polynomial to the estimated standard deviations, resulting in the noise characteristics overlaid in Fig. 3 as a solid black line. The modeling procedures we use assume that the device measurements have independent identically distributed (i.i.d) noise characteristics at all test points. To achieve this, we divide the measurements at any particular test point by the fitted noise characteristic.[4] When predicting the INL characteristic of a device, we reverse this division by a multiplication with the noise characteristic at each test point.

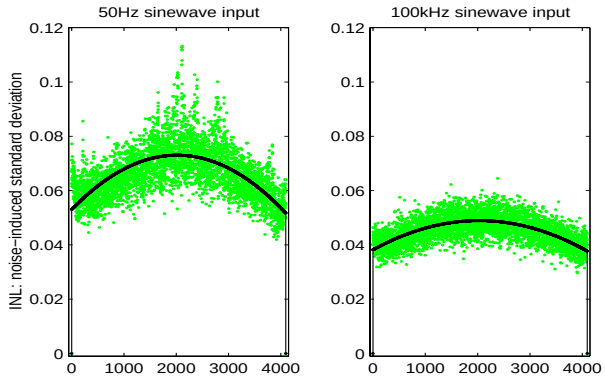

Fig. 3. Standard deviation of INL measurement versus code.

Test point selection is based on D-optimality [13], which minimizes the volume in the model parameter space that is caused by noisy measurements at the test points. A search algorithm based on QR-decomposition of the model matrix has been introduced in [14]. This algorithm yields n test points that are the necessary minimum to estimate the vector x in (1). To select more test points, we iteratively apply this algorithm to the model matrix A. After each iteration, the rows corresponding to the selected test points are filled with zeros, which causes the algorithm to ignore these test points in the next search iteration. In this manner, we select n, $2n$, $3n$,... test points until we reach the maximum of all available test points.

In Fig. 4, we plot for $n = 40$ the prediction error versus the number of test points. We observe that the

[4] Where the noise characteristic is zero, we divide by unity. This choice of scaling by unity does not affect our modeling procedures as the INL at the end points is zero by construction.

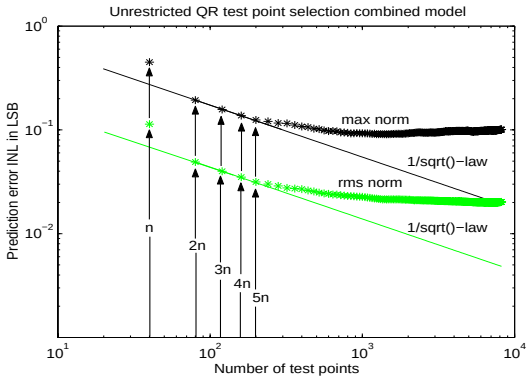

Fig. 4. Prediction error versus number of test points. Test point selection is based on the (unrestricted) QR-algorithm.

prediction error tends to decrease as the number of test points increases. A particularly steep decrease of the prediction error is observed when we increase the number of test points from the bare minimum of n to $2n$. When increasing the number of test points beyond this number, we have a lower bound [1] on the prediction error: multiplying the number of test points by k can decrease the prediction error by a factor of $\sqrt{k}$ at most. This "1/sqrt()-law" is indicated in the plot by a straight line due to the double-logarithmic scaling of the axis. As the plot shows, taking between $2n$ and $5n$ test points yields prediction errors close to the lower bound.

III. Test Point Selection Reviewed

So far, we have assumed that taking one test point is as costly as taking another. However, if we can restrict test point selection to the set of dynamic INL test points, where we use a 100 kHz sine-wave input, we realize that these measurements are performed with the same setup which is used for another ADC test: the Signal-to-Noise and Distortion (SNR+D) test. Thus, we might save test effort by using only one setup in production.

A plot of the percentage of test points selected by the QR-algorithm from the dynamic INL versus the total number of test points is shown in Fig. 5. In particular, for the total number of test points lying between $2n = 80$ and $5n = 200$, we observe that the QR algorithm selects mostly test points from the measurements performed with the 100 kHz input. This raises the question by how much the prediction error degrades if we restrict test point selection *a priori* to the dynamic INL. Restricting the set of selectable test points even further by excluding the top and bottom 100 codes, we can even re-use the measurements performed for the SNR+D test.

In Fig. 6, we compare the plot from Fig. 4 with the same plot of prediction error versus the number of test points under the *a priori* introduced restriction. For the number of test points between $2n$ and $5n$, the degradation of the prediction error is almost negligible.

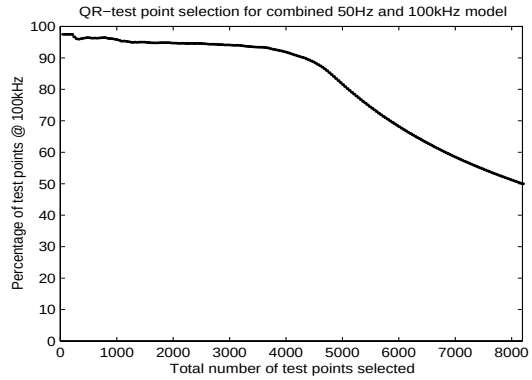

Fig. 5. Percentage of QR-selected dynamic INL test points versus total number of test points.

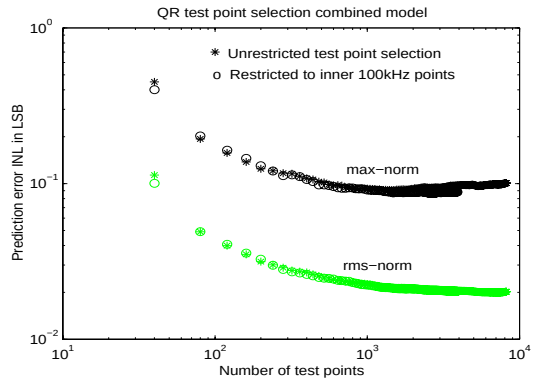

Fig. 6. Prediction error versus number of test points. Test points selection is based on QR-algorithm: (*) unrestricted and (o) restricted to code 100 through 3996 of dynamic INL.

In Table I, we present the prediction error for different *a priori* restricted sets of test points. This table clearly shows that the best result (in terms of $e_{\max}$ and $e_{\rm rms}$) is obtained when we restrict the measurements to the dynamic INL (code 100 through 3996). In particular, this set of test points can be measured using a large-scale 100 kHz sine-wave input which is also compatible with SNR+D testing, and thus, minimizes overall measurement effort for testing this ADC.

IV. Conclusions

In this work we have presented model-based testing of ADC nonlinearities. The model comprises static and dynamic error mechanisms present in the ADC we have used. However, the test point selection algorithm favored the less noisy measurements of the dynamic INL to estimate the model parameters. Based on this, we have introduced an *a priori* restriction on the usable set of test points. This restriction allows us to use the same measurement data of a converted 100 kHz sine-wave for both the INL and SNR+D test. As it turns out, from measurements under this dynamic test condition, the model yields even more accurate predictions of the static part of the INL than can be obtained from static INL measurements. This is due to a lower noise contribution of the test setup.

measure / predict	static INL	stat. & dyn.	dynamic INL
static INL	0.1104 0.0299	0.0895 0.0266	0.0855 0.0223
static & dyn. INL	0.1121 0.0275	0.0907 0.0213	0.0862 0.0207
dynamic INL	0.1032 0.0268	0.0806 0.0218	0.0769 0.0213

TABLE I. INL prediction error $e_{\max}$ (in black) and $e_{\rm rms}$ (in gray) based on measurements at set of test points selected by QR-algorithm with *a priori* restrictions.

References

[1] P.D. Capofreddi and B.A. Wooley. The use of linear models in A/D converter testing. *IEEE Trans. Circuits and Systems-I*, 44(12):1105–1113, December 1997.

[2] T. Kuyel. Linearity testing issues of analog to digital converters. In *Proc. ITC'99*, Int. Test Conf., pages 747–756. IEEE, October 1999.

[3] The Institute of Electrical and Electronics Engineers, Inc., New York. *IEEE-Std-1241 Draft*, March 2000. IEEE standard for terminology and test methods for analog-to-digital converters.

[4] J. Doernberg, H. Lee, and D. Hodges. Full speed testing of A/D converters. *IEEE J. Solid-State Circuits*, SC-19(6):820–827, December 1984.

[5] G.N. Stenbakken and T.M. Souders. Modeling and test point selection for data converter testing. In *ITC*, Int. Test Conf., pages 813–817, 1985.

[6] G.N. Stenbakken and T.M. Souders. Developing linear error models for analog devices. *IEEE Trans. Instr. Meas.*, IM-43(2):157–163, 1994.

[7] J. van Spaandonk. Application of the singular value decomposition to testing of analog circuits. In *Proc. IMSTW*, Int. Mixed-Signal Testing Workshop, pages 159–164, 1995.

[8] A. Wrixon and M. P. Kennedy. A rigorous exposition of the LEMMA method for analog and mixed-signal testing. *IEEE Trans. Instr. and Measurement*, IM-48(5):978–985, October 1999.

[9] C. Wegener, M. P. Kennedy, and B. Straube. Process deviations and spot defects: Two aspects of test and test development for mixed-signal circuits. *Journal of Electronic Testing Theory and Applications*, 17(5):409–416, October 2001.

[10] S. Cherubal and A. Chatterjee. Optimal INL/DNL testing of A/D converters using a linear model. In *Proc. ITC*, Int. Test Conf., pages 358–366, Oct. 2000.

[11] Gene H. Golub and Charles F. van Loan. *Matrix Computations*. Johns Hopkins Univ. Press, Baltimore, 3rd edition, 1996.

[12] A.A. Ding and J.T.G. Hwang. Prediction intervals, factor analysis models, and high-dimensional empirical linear prediction. *J. of the American Statistical Association*, 94(446):446–455, June 1999.

[13] Valerii V. Federov and Peter Hackel. *Model-Oriented Design of Experiments*. Number 125 in Lecture Notes in Statistics. Springer-Verlag, New York, 1997.

[14] G.N. Stenbakken and T.M. Souders. Test-point selection and testability measures via QR factorization of linear models. *IEEE Trans. Instr. Meas.*, IM-36(2):406–410, June 1987.